Application of different fatigue strength criteria to shot peened notched components. Part 1: Fracture Mechanics based approaches

Sara Bagherifard, Chiara Colombo, Mario Guagliano *

Poilitecnico di Milano, Department of Mechanical Engineering Via La Masa 1, 20156, Milan, Italy

Article history:
Received 4 July 2013
Received in revised form 20 October 2013
Accepted 20 October 2013
Available online 29 October 2013

1. Introduction

Shot peening (SP) is a well-known mechanical surface treatment generally applied to improve fatigue behavior of metallic components. During SP process, a large number of hard and almost spherical shots accelerated in peening device impact the surface of a work piece and cause local plasticity. It is known that SP is a considerably useful method to increase the roughness, improve fatigue properties, avoid fretting, wear and stress corrosion cracking. Final aim of the process is to create compressive residual stresses close to the surface and work-harden the same layer of material. These effects are very useful in order to totally prevent or greatly delay the failure of the part [1–3]. The schematic of the air blast shot peening equipment that is the standard apparatus for this treatment is illustrated in Fig. 1. Other types of plants can be used; the final effect on the treated surface is not varying with the technology used to accelerate the media.

Normally SP is reported to be more effective for fatigue strength improvement of components with geometrical discontinuities, with respect to smooth ones, mainly due to presence of high stress gradient [4–6]. This observation can be attributed to the fact that the high gradient just under the notch results in considerable decrease in the stress level, and at the same time the compressive residual stresses induced by SP help stopping and retarding crack propagation.

Fatigue strength assessment of structural components is an essential step within their design process. Application of experimental approaches to determine the S–N diagram of notched components under a wide range of loading conditions and notch effects requires an extremely high effort in terms of time and costs. To limit or eventually avoid the required experimental efforts, fatigue assessment criteria are generally used, even if the application of each criterion is mostly limited to particular loading condition or material range. That is to say a unique criterion able to cover all practical cases is not still available. Application of a criteria to shot peened parts is still more difficult due to the modifications induced by SP in the surface layer of the treated material. SP involves generation of compressive residual stresses, work hardening and surface topography alteration. Due to the complex nature of the phenomenon, it is not easy to find a universally accepted theoretical model for assessing the fatigue strength of shot peened components that can be sufficiently robust to deal with various conditions. Indeed, despite the importance of the stress concentration effect on fatigue strength, still an agreed set of standard methods for evaluating the effect of notches, holes, joints, defects and other stress-raisers is not available and there is not a commonly accepted fatigue assessment criterion in the literature to be applied to shot peened parts. Notwithstanding SP's widely recognized beneficial effects on fatigue strength, its contribution is

* Corresponding author.
E-mail addresses: sara.bagherifard@polimi.it (S. Bagherifard), chiara.colombo@polimi.it (C. Colombo), mario.guagliano@polimi.it (M. Guagliano).

Nomenclature

R	stress ratio
σ_{eff}	effective stress
$\Delta\sigma_0$	plain fatigue strength
L	material characteristic length
ΔK_{th}	range of the threshold value of the stress intensity factor
f_0	pulsating plain fatigue strength
f_{-1}	fully reversed plain fatigue strength
σ^{RS}	residual stress components
σ_m	mean stress component
α	material parameters
β	material parameters
σ_{VM}	Von-Mises stress
p_m	mean hydrostatic pressure
σ_{eq}	equivalent stress b_2 roughness coefficient
$\Delta\sigma_{g,th}$	threshold range of the gross nominal stress
α_γ	non-dimensional coefficient, dependent on component geometry, loading type and notch opening angle
a	reference dimension of a component, for example the notch depth
ã	degree of singularity of the stress distributions
$\Delta K^V_{i,th}$	threshold range of mode I notch-stress intensity factor
$\Delta\sigma_0$	range of the fatigue limit of the material
a^V_0	characteristic length parameter for a V-notched component
β_{LEFM}	coefficient that depends only on the notch opening angle

generally underestimated by the design codes; mainly due to the difficulties involved in correctly considering the peculiar effects of SP in fatigue strength assessments. For instance AGMA code for gears [7], that to the best knowledge of the authors is the only design code that considers quantitatively the SP contribution, has recognized that SP increases the fatigue strength of gears up to 25%, even if in many cases the actual improvement is more than this.

The present paper is aimed at critically reviewing the application of the most widely used fatigue criteria to shot peened notched specimens. The study is based on the results obtained for specimens with different notch geometries, applied loads and SP parameters. The considered criteria are divided in two major groups that have the potential to provide the design engineer with a practical tool to address the fatigue strength of shot peened material. The criteria considered in this study are mainly based on fracture mechanics and local stress approaches. Other criteria as the De los Rios [8] concepts are also helpful to understand the mechanisms through which SP influences the fatigue strength; however this criteria is not so practical to be used for notched components, since its implementation requires data and parameters that are not easily available for many materials and thus is not considered in the present paper. In this first part the fracture mechanics concept based approaches are discussed.

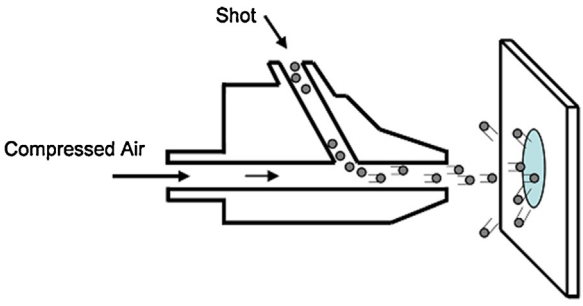

Fig. 1. Schematic illustration showing the equipment of air blast shot peening.

Theory of critical distance (TCD) [9–12], as the first approach, assumes fatigue strength can correctly be estimated only if the entire stress field damaging the fatigue process zone is correctly taken into account, suggesting to average the stress close to the stress concentrator apex over a material unit called as critical distance.

The second criteria is based on the statement that under appropriate conditions, notches can behave as cracks with the same depth and the fatigue limit can be estimated by means of linear elastic fracture mechanics [13]. A unified approach proposed by Atzori et al. [13] which substitutes the notch effect by an equivalent crack and estimates the fatigue limit for different stress raisers (i.e. defects, cracks, crack-like notches and blunt notches) was considered.

These criteria are applied to two different experimental campaigns that are subjected to rotating bending and axial fatigue tests. The comparison highlights the restrictions of each approach and the field in which they can be successfully applied; where possible, appropriate corrections are introduced in order to obtain a better agreement with the experimental results.

2. Fatigue assessment criteria

In this section a brief review of two fracture mechanics based methods applied for calculation of fatigue strength of notched components subjected to SP is provided.

2.1. Theory of critical distance (TCD)

Originally proposed by Neuber [9] and later simplified by Peterson [10], TCD implies that the maximum stress at the notch root is inappropriate for fatigue prediction in situations where the gradient of stress near the notch is high. Here we have considered the revision of Taylor to the TCD that is based on the calculation of the equivalent strength on a line (Line Method (LM)) [11]. LM method assumes that the notch fatigue response is governed by an effective stress, calculated through the material characteristic length, L, as a function of the stress field in the neighborhood of the notch tip.

According to the TCD, notched components are in their fatigue limit condition when the effective stress $\Delta\sigma_{eff}$, calculated by averaging an equivalent stress σ_{eq} along the notch bisector over the material characteristic length L, equals the plain fatigue strength, $\Delta\sigma_0$ (see Fig. 2).

$$S(L) = \frac{1}{2L}\int_0^{2L} \sigma_{eq} dy = \Delta\sigma_0 \tag{1}$$

where y is the local coordinate along the notch bisector with the origin lying on the notch apex. The material characteristic length, L, can be calculated as follows [12,14]:

$$L = \frac{1}{\pi}\left(\frac{\Delta K_{th}}{\Delta\sigma_0}\right)^2 \tag{2}$$

where ΔK_{th} is the range of the threshold value of the stress intensity factor and, again, $\Delta\sigma_0$ is the plain fatigue limit of the material (both determined under the same load ratio, R, applied to the specimen).

The TCD approach can be applied to assess fatigue strength of shot peened notched components considering the effective stress $\Delta\sigma_{eff}$ according to the Sines criterion and residual stresses as mean

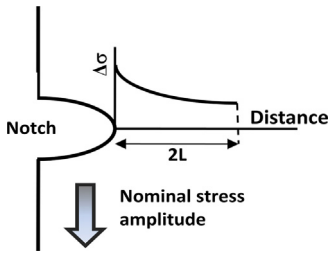

Fig. 2. Schematic plot of the stress distribution in the vicinity of the notch tip and the distance over which the TCD method integrates the stress.

stresses superimposed to the oscillating stresses introduced by the external cyclic load [15].

2.2. Atzori approach

Smith and Miller [16], Taylor [17], Taylor et al. [18] and Wang et al. [19] have shown that in certain circumstances, a notch of depth D can behave as a crack of the same depth. Fatigue failure is supposed to occur if the stress intensity range for the equivalent crack exceeds the material's threshold value, ΔK_{th}.

Atzori et al. [13] presented a unified treatment of U and V notches with arbitrary notch opening angle and notch tip radius subjected to prevailing mode I fatigue loadings. Following this approach, the fatigue limit range of a notched component can be estimated according to Eq. (3), where $\Delta\sigma_{g,th}$ is the range of the fatigue limit of the notched component, α_γ is a parameter that depends upon the position of the notch in the component, a is the notch depth, γ is a parameter that depends on the angle of opening of the notch, while $\Delta K^V_{I,th}$ and a^V_0 are given in Eqs. (4) and (5) respectively:

$$\Delta\sigma_{g,th} = \frac{\Delta k^V_{I,th}}{\sqrt{\pi}(\alpha_\gamma^{1/\gamma} a + a_0^V)^\gamma} \tag{3}$$

$$\Delta K^V_{I,th} = \beta_{LEFM}\,\Delta\sigma_0^{(1-2\gamma)}\,\Delta K_{th}^{2\gamma} \tag{4}$$

$$a_0^V =\geq \left(\frac{\Delta K^V_{I,th}}{\sqrt{\pi}\Delta\sigma_0}\right)^{1/gg} \tag{5}$$

In Eqs. (4) and (5) $\Delta\sigma_0$ and ΔK_{th} are correspondingly the range of the fatigue limit of the material and the threshold stress intensity range and β_{LEFM} is a coefficient that depends only on the notch opening angle [13]. Atzori et al. [13] have demonstrated this equation to be valid for K_t ranging from 3 to 30. Eq. (3) has been validated for different low and high strength steels and Al alloys [13].

3. Experimental procedure

The mentioned fatigue assessment criteria were applied to two different fatigue test lots consisting of rotating bending tests (RBT) and axial tests (AT), both performed on shot peened notched specimens. In both cases the tests were performed following the Staircase procedure [20] and the fatigue strength corresponding to a fatigue life of 3 million cycles was calculated through the Hodge–Rosenblatt approach [21]. The fatigue test data were elaborated based on the ASTM standard E739-10 [22]. Details of the material characteristics and the surface treatment applied to each series are as following.

For the RBT series, low alloy steel (40NiCrMo7, UNI 7845) smooth and notched specimens were shot peened using three different SP sets of parameters. The material nominal chemical composition and the treatment parameters are respectively presented in Tables 1 and 2.

The geometries of the smooth and notched specimens used for RBT, designed in accordance with ISO 1143 [23], are shown in Fig. 3. The stress concentration factor of the notch for all series is $K_t = 2$ that is common in many machine elements such as shafts and springs.

AT were also performed on differently shot peened series of notched steel specimens. The material under investigation is the steel normally used in pipeline applications named as A95. The choice of the specimen geometry stress concentration factor of $K_t = 5.9$ is based on the geometry of the threaded components commonly used in pipelines. Specimen geometry is shown in Fig. 4 and the applied SP parameters are presented in Table 3.

To study the residual stresses, X-ray diffraction (XRD) analysis was performed on the specimens using an AST X-Stress 3000 X-ray diffractometer (radiation Cr Kψ, circular irradiated area of 1 mm diameter, $\sin^2\psi$ method, diffraction angles scanned between −45 and 45). Measurements were carried out in depth step by step removing a very thin layer of material using an electro-polishing device in order to obtain the in-depth trend of residual stresses. A solution of acetic acid (94%) and perchloric acid (6%) was used for electro-polishing. Apart from residual stresses, FWHM parameter (full width half maximum) is also measured by the X-ray diffractometer. FWHM represents the full width of the diffraction peak at half of the maximum intensity. It is considered as an index of the distortion of the crystal grain, the density of dislocations in the crystal lattice and micro residual stresses of type II. In this work, FWHM is taken as an indicator for work hardening of the material [24]. It is to be mentioned that the peak width broadening induced by instrument has been accounted for, by calibrating the device with a strain free standard sample of the same material group.

Surface roughness of the treated specimens was measured and compared to that of the NP series. A Mahr profilometer PGK, that is an electronic contact instrument, equipped with MFW-250 mechanical probe and a stylus with tip radius of 2 μm was used to trace the surface profiles. Surface roughness data were obtained

Table 1
Nominal chemical composition of 40NiCrMo7 steel in mass density.

C	Si_{max}	Mn	P_{max}	S_{max}	Cr	Mo	Ni
0.37–0.44 ±0.02	0.15–0.40 ±0.03	0.50–0.80 ±0.04	0.035 +0.005	0.035 ±0.005	0.60–0.90 ±0.05	0.20–0.30 ±0.03	1.60–1.90 ±0.05

Table 2
Aspects of the SP treatment applied to RBT specimens.

Series	Shot type and diameter (mm)	Almen intensity (0.0001 in.)	Coverage%
RBT-SP1	Z100 (ceramic, $\phi = 0.1$)	10–12 N	100
RBT-SP2	S110 (steel, $\phi = 0.3$)	4–6 A	100
RBT-SP3	S170 (steel, $\phi = 0.43$)	10–12 A	100

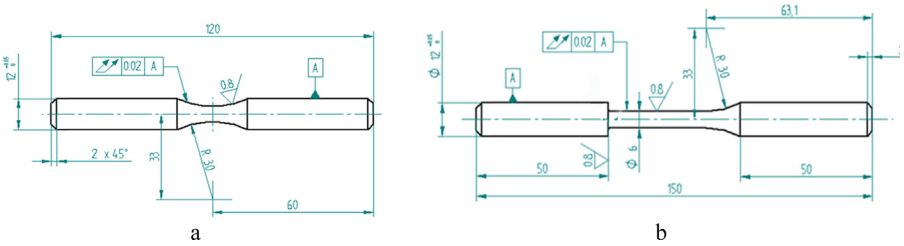

Fig. 3. RBT fatigue specimens' geometry (a) smooth specimen (b) notched specimen.

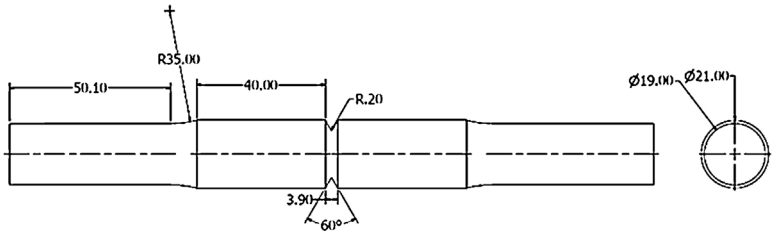

Fig. 4. Geometry of AT specimen.

Table 3
Aspects of the SP treatment applied to AT series.

Treatment	Shot type and diameter (mm)	Almen intensity (0.0001 in.)	Coverage%
AT-SP1	S70 (steel, $\phi = 0.18$)	8–10 N	400
AT-SP2	S70 (steel, $\phi = 0.18$)	12–14 N	100
AT-SP3	S70 (steel, $\phi = 0.18$)	8–10 A	100

by performing three measurements in three distinct areas of each individual specimen to consider the variability of surface roughness by location.

4. Experimental results

4.1. Fatigue tests

4.1.1. Rotating bending test series

Rotating bending fatigue tests (stress ratio $R = \sigma_{min}/\sigma_{max} = -1$) were carried out at room temperature on the as-received not peened (NP), and the shot peened series. Fatigue strength corresponding to a fatigue life of 3 million cycles, calculated using Hodge–Rosenblatt [21], method are presented in Table 4. The fatigue test data, presented in Fig. 5, were analyzed based on the ASTM standard E739-10 [22] to obtain the S-N diagram for different cases with a failure probability of 50% in bi-logarithmic scale. The results indicate that in all cases SP induces fatigue strength improvement, whereas the enhancement is becomes more remarkable by increasing the Almen intensity. The fatigue strength improvement as expected is more notable for notched series (Table 5).

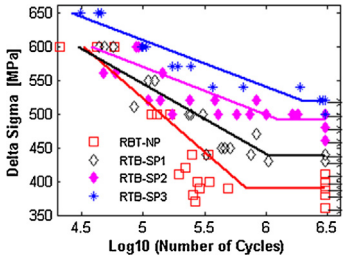

Fig. 5. The S–N diagram for notched RTB series.

4.1.2. Axial test series

Pull–push axial fatigue tests were conducted at room temperature on NP series as well as all the described series of shot peened specimens. The tests were carried out in load control mode with stress ratios of $R = 0.1$. The fatigue test data was analyzed based on the ASTM standard E739-10 [22] to obtain the S–N diagram for different cases with a failure probability of 50% in bi-logarithmic scale, as presented in Fig. 6.

4.2. Analysis of the residual stress profile

Residual stress and FWHM distribution for all the series of specimens measured in the axial direction are presented in Fig. 7. Increasing the Almen intensity shifts the maximum value of com-

Table 4
Fatigue test results for RTB series.

Series	Fatigue limit (MPa)	
	Smooth specimens	Notched specimens
RBT-NP	602	390
RBT-SP1	705	438
RBT-SP2	676	492
RBT-SP3	712	518

Table 5
Fatigue test results for AT series.

Series	Fatigue limit (MPa)
AT-NP	170
AT-SP1	212
AT-SP2	212
AT-SP3	220

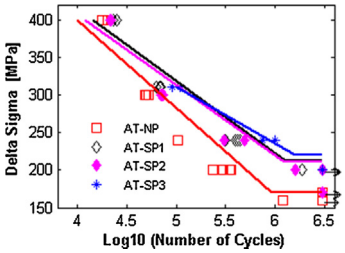

Fig. 6. The S–N diagram for AT series.

pressive residual stresses to higher depths. The surface value of FWHM is growing with increasing kinetic energy of the SP process. This issue has been validated also numerically in authors' previous study [25]. It is to be noted that the thickness of the work hardened layer can be estimated as the thickness of the layer, which shows considerably increased FWHM values in comparison with the core material. As the results demonstrate this thickness is slightly increasing by enhancing the Almen intensity of the SP process.

4.3. Roughness measurements

The average of the obtained results is presented in Tables 6 and 7 for RBT and AT series respectively.

Table 6
Surface roughness parameters of RBT series.

Treatment	R_a (μm)	R_z (μm)	R_t (μm)
RBT-NP	1.37	5.84	6.21
RBT-SP1	1.49	8.50	9.80
RBT-SP2	1.73	9.28	12.36
RBT-SP3	2.35	12.07	14.32

Table 7
Surface roughness parameters of AT series.

Treatment	R_a (μm)	R_z (μm)	R_t (μm)
AT-NP	2.92	11.37	12.00
AT-SP1	2.30	13.41	17.63
AT-SP2	1.17	7.45	9.32
AT-SP3	4.37	23.43	28.31

5. Application of the criteria on AT and RBT series

5.1. Theory of critical distance (TCD)

The LM method proposes the critical condition to be achieved, as the effective stress, averaged over a distance equal to $2L$ reaches the smooth specimen fatigue strength $\Delta\sigma_0$ (Eq. (1)):

Equivalent stress can be calculated using the Sines criterion [26] in order to consider the biaxial state of stress induced by SP. The residual stresses can be as mean stresses superimposed to the stresses due to the external cyclic load [15]. Sines criterion includes the Von-Mises stress amplitude $\sigma_{VM}(\sigma_a)$ and the mean hydrostatic pressure p_m in a linear equation:

$$\sigma_{VM}(\sigma_a) + \alpha \times p_m = \beta \tag{6}$$

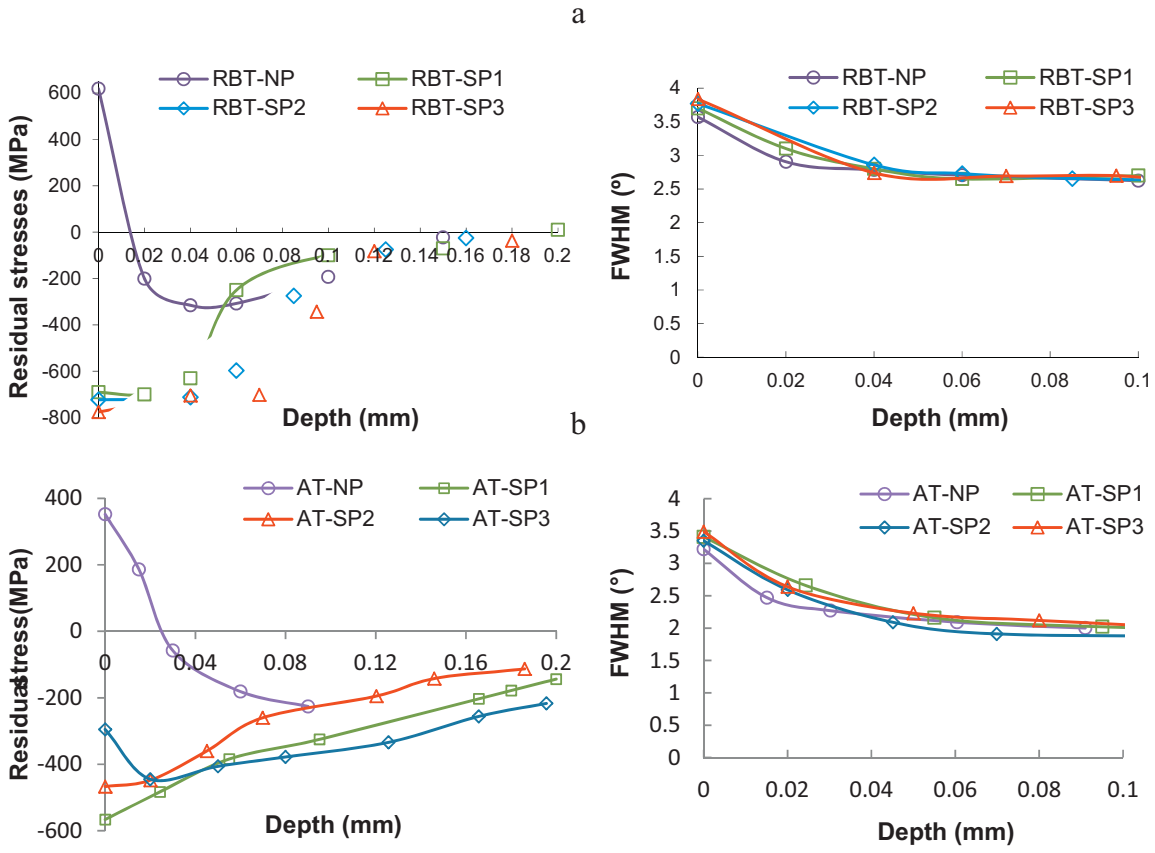

Fig. 7. Distribution of the residual stresses and FWHM obtained by XRD for (a) RBT series (b) AT series.

Table 8
The parameters used for calculation of RTB series' fatigue limit.

ΔK_{th} (MPa$\sqrt{m}$) [31]	$\Delta\sigma_0$ (MPa) (experiment)	L (μm) (Eq. (2))	f_{-1} (MPa)	f_0 (MPa)	Yield stress (MPa)	Tensile strength (R_m) (MPa)
11	1204	27	565	384	835	1200

By implementing the criterion of Sines in Eq. (6) the following equation is obtained:

$$\frac{1}{2L}\int_0^{2L}(\sigma_{VM}(\sigma_a)+\alpha\times p_m)dy=\Delta\sigma_0 \tag{7}$$

where $\Delta\sigma_0$ is the plain fatigue strength; α and β are material parameters that refer to the NP conditions according to the assumption that the material's work hardening introduced by the SP exerts a negligible influence on the fatigue resistance [15]. In case of $R=-1$, the mean hydrostatic pressure, assuming that the residual stresses induced by SP are bi-axial, can be defined as:

$$p_m=\frac{(\sigma_{1,m}+\sigma_{2,m}+\sigma_{3,m})+(\sigma_1^{Rs}+\sigma_2^{Rs}+\sigma_3^{Rs})}{3}=\frac{\sigma_1^{RS}+\sigma_2^{RS}}{3} \tag{8}$$

where σ_1^{RS} and σ_2^{RS} are the components of residual stress introduced by SP and σ_m, α and β are identified from two independent fatigue tests: f_{-1} and f_0 that are fully reversed and pulsating plain fatigue strength for a given number of cycles to failure, respectively.

$$\alpha=3\left(\frac{f_{-1}}{f_0}-1\right) \tag{9}$$

$$\beta=f_{-1} \tag{10}$$

5.1.1. RBT series

The stress distribution induced by the external load for the as-received specimen is calculated through a finite element analysis. The fatigue limits f_{-1} and f_0 are taken from the rotating bending fatigue tests performed on the smooth specimens. Thus the amplitude of the applied bending stress σ_a, is the only unknown of Eq. (7).

TCD approach, not being developed for shot peened specimens, does not take account of surface roughness which is a well-recognized side effect of SP that normally leads to fatigue strength reduction [27,28]. Since relatively high surface roughness values have been observed on all shot peened series, a roughness factor that is ratio of surface roughness coefficient (C_s) for peened specimen to that of the NP specimen of the same material has been introduced in to the calculations based on surface factor diagrams provided by Buch [29].

A further modification of Eq. (1) is to apply a work hardening coefficient introduced by Fernandez Pariente and Guagliano [30]. FWHM is related to the grain distortion and to the dislocation density and can be used as an index of surface hardening to compare the state of different surfaces. Considering the negligible depth of X-ray penetration, The FWHM value measured by XRD refers only to the surface and does not include a finite thickness of material, as microhardness does, thus it can be directly related to the effect of the applied surface treatment.

The parameters used for the calculation are presented in Table 8 and the results obtained through the application of the method considering the modifying factors are presented in Table 9.

Application of the correction coefficients, as reported in Table 9, reduces the maximum overestimating error of around 45% to a maximum of 34%. This overestimation can be attributed to the hydrostatic pressure defined in Eq. (8); since the mean hydrostatic pressure includes two components of residual stresses induced by SP. One component is in the same plane of the stresses caused by application of the external load; while the other lays in a plane perpendicular to the applied load. Considering that the external load is uni-axial, the two components of residual stress will not have the same effect; thus it seems to be more appropriate to consider just the component of residual stresses that is in the direction of the external load. Hence the calculations are repeated applying the LM method according to the original approach of Taylor [11] and implementing the criterion of Sines, considering just one component of σ_1^{RS} and eventually introducing the correction factors to consider the effect of work hardening and surface roughness; the following result are obtained (Table 10).

Table 9
Fatigue limit of RTB series (TCD (multi-axial stress) vs. experimental data).

Treatment	Calculated fatigue limit (MPa)	Experimental data (MPa)	Error %
RBT-SP1	514	438	17%
RBT-SP2	662	492	34%
RBT-SP3	625	518	20%

Table 10
Fatigue limit of RTB series (TCD (uni-axial stresses) vs. experimental data).

Treatment	Calculated fatigue limit (MPa)	Experimental data (MPa)	Error %
RBT-SP1	417	438	−5.03%
RBT-SP2	494	492	0.40%
RBT-SP3	463	518	−11.87%

It is observed that the error caused through considering a single component of the hydrostatic pressure is much lower than that generated by considering both components. It seems that in this case, in which the external load is uni-axial, it is more appropriate to implement only the component of the residual stress coplanar with the component given by the external load.

5.1.2. AT series

The same approach is applied in case of AT series; axial fatigue tests performed with stress ratio $R\neq-1$, the mean hydrostatic pressure, assuming that the residual stresses induced by SP are biaxial, is defined as:

$$p_m=\frac{(\sigma_{1,m}+\sigma_{2,m}+\sigma_{3,m})+(\sigma_1^{Rs}+\sigma_2^{Rs}+\sigma_3^{Rs})}{3}=\frac{\sigma_{1m}+\sigma_1^{RS}+\sigma_2^{RS}}{3} \tag{11}$$

where σ_1^{RS} and σ_2^{RS} are the components of residual stress introduced by SP; and σ_{1m} is the component of the mean stress due to the external load. Following the discussion made in Section 5.2.1, just the component of residual stress in the plane of the external load that is σ_1^{RS} was used in the calculation of mean hydrostatic pressure. The single component of σ_{VM} was calculated from a finite element model and then normalized to the maximum value of stress. The parameters used for fatigue limit calculation are presented in Table 11. The results after introduction of correction factors to consider the phenomenon of surface hardening and deterioration of surface roughness are presented in Table 12.

Also in case of AT series the fatigue limit calculated by considering just the component of the hydrostatic pressure that is in the same direction of the external load, provides a better agreement with experiments; the data obtained by considering both components of hydrostatic pressure are not reported for the sake of conciseness.

In the end, it is observed that for both series of tests the maximum error from application of TCD method is slightly greater than 10% and therefore very low.

Table 11
The parameters used for calculation of AT series' fatigue limit.

ΔK_{th} (MPa$\sqrt{m}$) [32]	$\Delta\sigma_0$ (MPa)	L (μm) (Eq. (2))	f_{-1}(MPa)	f_0 (MPa)	Yield stress (MPa)	Tensile strength (R_m) (MPa)
13	822	80	411	273	728	810

Table 12
Fatigue limit of AT-A95 series (TCD (uni-axial stresses) vs. experimental data).

Treatment	Calculated fatigue limit (MPa)	Experimental data (MPa)	Error %
AT-SP1	236	212	10%
AT-SP2	210	212	−0.95%
AT-SP3	226	220	2.65%

Table 13
the parameters used for calculation of AT series' fatigue limit.

ΔK_{th} (MPa$\sqrt{m}$) [32]	$\Delta\sigma_0$ (MPa)	$\Delta K^V_{i,th}$ (Eq. (4)) (MPa$\sqrt{m}$)	a^V_0(Eq. (5)) (μm)	$\Delta\sigma_{g,th}$ (Eq. (3)) (MPa)
13	822	14.85	82	63

5.2. Atzori approach

Given the geometry of the RBT specimens shown in Fig. 3, the notch falls into the category of the blunt notch with the stress concentration factor out of the range considered by Atzori et al. In light of this observation, the approach of Atzori et al. [13] is not applied to RBT series.

For AT series, the approach described in Section 2.2 is followed. The coefficient β_{LEFM} for the geometry of the reference specimen, with an opening angle of 60°, is equal to 1.03, according to the tables provided in [13], while the notch depth, a, is equal to 3.15 mm; α_γ is the geometric coefficient of stress intensity factor that takes the position of the crack within the component into account; while γ is related to the opening angle of the notch and the reference geometry is 0.4878 [13]. The parameter α_γ can be determined by accurate FE analyses where the notch is modeled as a crack having the same depth; appropriate data is available for standard geometries and loading conditions in fracture mechanic handbooks (Table 13).

The fatigue limit calculated from Eq. (3), was then corrected to consider the effect of stress ratio (R = 0.1 for AT series) and also the effect of residual stress acting as mean stress, by using Haigh diagram with Morrow approximation. The obtained result was again modified by applying the coefficients that consider the effect of work hardening and increased surface roughness due to the SP treatment as defined in Section 5.1.1. Table 14 shows the obtained results.

Although this method suitably considers the presence of the residual stresses in fatigue life assessment, it provides very approximate estimation of the experimental data, especially for SP processes that have higher impact energies. Indeed the fatigue strength obtained experimentally for the three series of specimens are quite alike indicating of the minor effect of different residual stress distributions. This issue can be attributed to the geometrical effects of the notch that might have resulted in relaxation of residual stresses developed through different shot peening treatments.

Table 14
Fatigue limit of specimens AT-A95 following the Atzori et al. approach.

Treatment	Calculated fatigue limit (MPa)	Experimental data (MPa)	Error %
AT-SP1	204	212	−3.9%
AT-SP2	180	212	−17.7%
AT-SP3	156	220	−29%

The partial relaxation of residual stresses on notched components under fatigue loading has been verified in previous studies [33].

6. Summary and conclusions

Two fracture mechanics based methods proposed for fatigue strength assessment of notched shot peened components were critically assessed and applied to different sets of specimens. The results are compared with the experimental test data. On the basis of the results the following conclusions can be drawn:

Coefficients of roughness and work hardening, respectively defined in order to take into account the surface roughness alteration and work hardening induced by shot peening treatment were implemented in the calculation of fatigue strength for both approaches.

The theory of critical distance with the implementation of the criterion of Sines is able to accurately consider the effect of the compressive residual stress introduced by shot peening as well as the effect of the mean stress component derived from the application of external load. It provides good correspondence with experimental data.

The Atzori et al. method requires the knowledge of the axial fatigue limit of the specimen and the threshold stress intensity range, in addition to a finite element analysis for determining the geometrical coefficient of stress concentration factor. The obtained results are quite conservative in predicting the fatigue limit of shot peened notched components with an underestimation of almost 30%.

Both methods require material parameters that can be extracted from simple tests. Although the intricacy of ΔK_{th} determination for specific materials for Atzori et al. method can be in some way limiting for practical applications.

Both methods require the determination of stress distribution induced by the external load, in correspondence to the notch; thus necessitate implementation of finite element analysis with very precise and fine mesh definition that in turn may markedly increase the computation time and costs.

Regarding the theory of critical distance approach in the case of uni-axial external stress, considering both components of residual stress induced by shot peening in Sines criterion leads to an overestimation of the result, while the error is greatly reduced by considering only the component of residual stress in the same direction of the external load.

To come to the point, the results indicate that the critical distance theory is able to get results closer to the experimental data probably since it considers the integral of the stress along a critical distance, thus being less sensitive to the unavoidable errors induced by experimental measurements. Therefore it provides a more robust solution to alterations of peening condition and measurement errors.

References

[1] J.O. Almen, P.H. Black, Residual Stresses and Fatigue in Metals, McGraw-Hill Publ. Company, 1963.
[2] K.J. Marsh, Shot Peening: Techniques and Applications, EMAS, London, 1993.
[3] V. Schulze, Modern Mechanical Surface Treatment, States, Stability, Effects, Wiley-VCH, 2006.
[4] H.O. Fuchs, The effect of self stresses on high cycle fatigue, J. Test. Eval. ASTM 10 (4) (1982) 168–173.
[5] W.J. Harris, Metallic Fatigue, Pergamon New, 1961.
[6] H.O. Fuchs, R.I. Stephens, Metal Fatigue in Engineering, John Wiley and Sons, 1980.
[7] AGMA 87FTM13, A Concept for Using Controlled Shot Peening Original Gear Design, American Gear Manufacturers Association, 1987.
[8] A. Navarro, E.R. De Los Rios, Short and long fatigue crack growth: a unified model, Philos. Mag. A (1988) 15–36.
[9] H. Neuber, Theory of Notch Stresses: Principles for Exact Calculation of Strength with Reference to Structural Form and Material, 2nd ed., Springer Verlag, Berlin, 1958.
[10] R.E. Peterson, Notch-sensitivity, in: G. Sines, J.L. Waisman (Eds.), Metal Fatigue, McGraw Hill, New York, 1959, pp. 293–306.
[11] D. Taylor, The theory of critical distances, Eng. Fract. Mech. 75 (2008) 1696–1705.
[12] L. Susmel, The theory of critical distances: a review of its applications in fatigue, Eng. Fract. Mech. 75 (2008) 1706–1724.
[13] B. Atzori, P. Lazzarin, G. Meneghetti, A unified treatment of the mode I fatigue limit of components containing notches or defects, Int. J. Fract. 133 (2005) 61–87.
[14] M.H. El Haddad, T.H. Topper, K.N. Smith, Fatigue crack propagation of short cracks, J. Eng. Mater. Technol. (ASME Trans.) 101 (1979) 42–45.
[15] M. Benedetti, V. Fontanari, C. Santus, M. Bandini, Notch fatigue behaviour of shot peened high-strength aluminium alloys: Experiments and predictions using a critical distance method, Int. J. Fatigue 32 (2010) 1600–1611.
[16] R.A. Smith, K.J. Miller, Prediction of fatigue regimes in notched components, Int. J. Mech. Sci. 20 (1978) 201–206.
[17] D. Taylor, Geometrical effects in fatigue: a unifying theoretical model, Int. J. Fatigue 21 (1999) 413–420.
[18] D. Taylor, W. Zhou, A.J. Ciepalowicz, J. Devlukia, Mixed-mode fatigue from stress concentrations: an approach based on equivalent stress intensity, Int. J. Fatigue 21 (1999) 173–178.
[19] G. Wang, D. Taylor, B. Bouquin, J. Devlukia, A. Ciepalowicz, Prediction of fatigue failure in camshaft using the crack modelling method, Eng. Fail. Anal. 7 (2000) 189–197.
[20] W. Dixon, F. Massey, Introduction to Statistical Analysis, McGraw-Hill, 1969.
[21] K.A. Brownlee, J.L. Hodges, J.R.M. Rossenblatt, The up-and-down method with small samples, J. Am. Stat. Assoc. 48 (1953) 262–277.
[22] ASTM Standard E739-10, Standard Practice for Statistical Analysis of Linear or Linearized Stress Life (S-N) and Strain Life (ε-N) Fatigue Data, 2010.
[23] ISO 1143 Metallic Materials – Rotating Bar Bending Fatigue Test, 2010.
[24] S. Bagherifard, M. Guagliano, Fatigue behavior of a low-alloy steel with nanostructured surface obtained by severe shot peening, Eng. Fract. Mech. 81 (2012) 56–68.
[25] S. Bagherifard, R. Ghelichi, M. Guagliano, A numerical model of severe shot peening (SSP) to predict the generation of a nanostructured surface layer of material, Surf. Coat. Technol. 204 (2010) 4081–4090.
[26] G. Sines, Behaviour of Metals Under Complex Static and Alternating Stresses, McGraw-Hill, New York, 1959.
[27] S. Bagherifard, R. Ghelichi, M. Guagliano, Numerical and experimental analysis of surface roughness generated by shot peening, Appl. Surf. Sci. 258–18 (2012) 6831–6840.
[28] S. Bagherifard, I. Fernandez-Pariente, R. Ghelichi, M. Guagliano, Fatigue behavior of steel notched specimens with nanocrystallized surface obtained by severe shot peening, Mater. Des. 45 (2013) 497–503.
[29] A. Buch, Fatigue Strength Calculation, Trans Tech, Switzerland, 1988.
[30] I. Pariente Fernandez, M. Guagliano, About the role of residual stress and surface work hardening on fatigue ΔK_{th} of a nitrided and shot peened low-alloy steel, Surf. Coat. Technol. 202 (2008) 3072–3080.
[31] The Ncode Book of Fatigue Theory, Ncode Techincal Reference Book V.5.3, 2000.
[32] Politecnico di Milano, Internal Report, 2009.
[33] K. Miková, S. Bagherifard, O. Bokuvka, M. Guagliano, L. Trško, Fatigue behavior of X70 microalloyed steel after severe shot peening, Int. J. Fatigue 55 (2013) 33–42.